Yang and Jin *J Infrastruct Preserv Resil* (2023) 4:10
https://doi.org/10.1186/s43065-023-00076-7

Journal of Infrastructure Preservation and Resilience

RESEARCH Open Access

Numerical analysis on seismic behavior of the assembled modular steel plate shear wall with inclined slots

Shengchao Yang[1,2] and Shuangshuang Jin[1,2*]

Abstract

This paper proposes a novel multi-grids steel plate shear wall with inclined slots (called MSPSW). This MSPSW composed of the steel plates with inclined slots, precast concrete panels, the transverse and longitudinal (T&L) connecting stiffeners, and external frame components. Smaller single plates can be used in the design and installation process since the space size of individual frames inside the frame is reduced as a result of the T&L connecting stiffeners. The direction of inclined slots in the adjacent grids is opposite, which makes the lateral resistance and stiffness close to symmetry. Numerical analysis is conducted to evaluate the seismic behavior. With the correct finite element model, finite element analysis is performed on the key parameters of MSPSW, such as the cross-sectional dimension of T&L connecting stiffeners, the thickness of steel plate, the width of inclined slots and the width of plate slot strips. The Mises distribution and development regular pattern of MSPSW are also explored. The FE numerical analysis discovered that the MSPSW increased the bearing capacity and energy consumption capacity of the members due to the installation of T&L connecting stiffeners. Additionally, the thickness required for concrete panels is lowered when the components are subjected to cyclical loads. Finally, the internal force development curves in frame beams and columns are extracted, it can be found that the internal forces become smaller, which weakens the demand of frame members. The theoretical calculation formulas of the maximum internal forces of frame beams and columns are provided.

Keywords Steel plate shear wall, Inclined slots, Multi-grids, Numerical analysis, Parametric analysis, Internal force analysis

Introduction

Lateral loads, such as wind loads and seismic loads, are frequently the main considerations in the design of high-rise building structures. In the 1970s, steel plate shear walls (SPSW) made their debut. It is very resistant to horizontal loads as a member that resists lateral forces. In high-rise buildings, it is extensively employed because of its good economic applicability. [1, 2]. In earlier studies on SPSWs, inner steel plates were thickened or stiffened to ensure that the SPSWs would function without buckling. Wagner [3] was the first to notice the comparatively thin steel plate's post-buckling behavior. A series of "folds" would form in the steel plate's diagonal direction after the steel plate displayed local buckling under a light horizontal force. Thorburn et al. [4] found in the early 1980s that unreinforced SPSWs can resist lateral loads via the diagonal tension field of the steel plates. Elgaaly et al. [5, 6], Lubell et al. [7], Park et al. [8–10], Qu et al. [11] conducted many experiments on the unstiffened SPSWs. According to the test results, at low load levels, the diagonal tension band created by shear buckling resists the lateral force, and the energy is released by the deformation

*Correspondence:
Shuangshuang Jin
jinshuangshuang@cqjtu.edu.cn
[1] State Key Laboratory of Mountain Bridge and Tunnel Engineering, Chongqing Jiaotong University, Chongqing, China
[2] School of Civil Engineering, Chongqing Jiaotong University, Chongqing, China

generated by the steel plate's buckling.However, the strength and stiffness of the border columns have a major role in the post-buckling performance of unreinforced SPSWs. When the boundary column prematurely fails before the SPSWs, the shear wall could not be fully developed. Thereafter, design requirements of boundary members have been provided in AISC 341 [12] and JGJ/T 380–2015 [13], the boundary columns required larger sizes to meet the minimum requirements.

Researchers from different nations have proposed and studied a variety of SPSWs to weaken the interaction between the edge frame column and the inner core steel plate [14–22]. Recently, a buckling-restrained SPSW with inclined slots has been proposed [23, 24]. By changing parameters such the number of slots (n) and the width of the steel strip (b), excessive forces on nearby border elements can be decreased. As shown in Fig. 1, the suggested SPSW is made up of a steel plate with inclined slots and two buckling-restrained concrete panels.

The inner steel plates for the above slotted SPSW are normally large in size, resulting in high manufacture and transportation costs, and the requirements for the buckling-restrained concrete panel are also greater. With these considerations, a new type of MSPSW is proposed in this study. By installing T&L connecting stiffeners on the basis of slotted SPSW, the entire frame space is divided into several grids. The MSPSW consists of the inner slotted steel plates sandwiched between precast concrete panels, the T&L connecting stiffeners and boundary frame. The steel plates with different inclined slots directions are installed in the small grids, which are divided by the frame and connecting stiffeners. In this paper, pushover analyses are carried out on finite element models of the MSPSWs created by ABAQUS software in order to understand the mechanical characteristics of the MSPSW under the horizontal loads. Through parametric analysis under lateral forces, certain significant influencing parameters are studied, including the thickness of the steel plate, the width of the inclined slots, the width of the slot strips, and the section size of the T&L connecting stiffeners. Furthermore, the internal force development of frame beams and columns under horizontal loads with different IDA is also explored, the influence of setting T&L connecting stiffener is carried out, and the theoretical formulae of the boundary columns are provided finally.

Configuration of the MSPSW

Figure 2 depicts the proposed MSPSW's configuration. Through boundary members and the T&L connecting stiffeners, the frame space is refined into a plurality of small grids, steel plates with different slots directions are installed in the grids. Precast restrained concrete panels are provided on both sides of the slotted steel plate, and the concrete panels are bolted to each other. Since the inclined slots are arranged in two different directions perpendicular to each other, under shear loads, the inclined strips of different orientations are subjected to different stress states. When the slotted steel plate in one grid is compressed under the cyclic load, steel plate in adjacent grids is tensioned, resulting in stable cyclic response and symmetric shear strength. The T&L connecting stiffeners are made of H-beam, which are connected with frame beams and columns by welding or bolting. Due to the existence of T&L connecting stiffeners, the out-of-plane stiffness of MSPSW is increased to a certain extent. Angles are set in the boundary members and the T&L connecting stiffeners to realize the bolt connection between the embedded steel plate and surrounding components. Appropriate clearances between the concrete panels and the surrounding elements should be allowed in order to prevent the MSPSW's concrete slab from participating in the resistance of horizontal loads under large displacements.

The size of a single embedded steel plate is decreased because the frame area is divided into multiple tiny grids. The T&L connecting stiffeners lessen the need for the buckling-restraint concrete panel while improving the overall out-of-plane stiffness of the MSPSW. The dimensions of the T&L connecting stiffeners and slotted steel plate can be combined flexibly to suit the necessary specifications for the buildings' structural layout. Small size

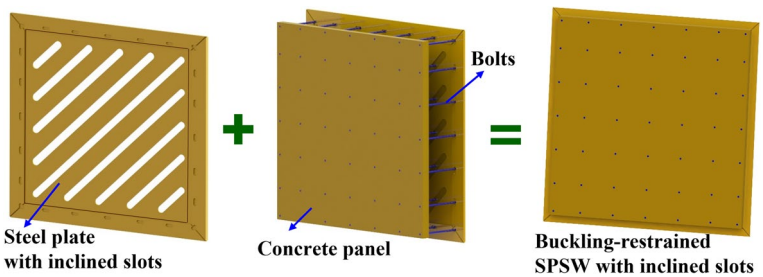

Fig. 1 Configuration of the slotted SPSW

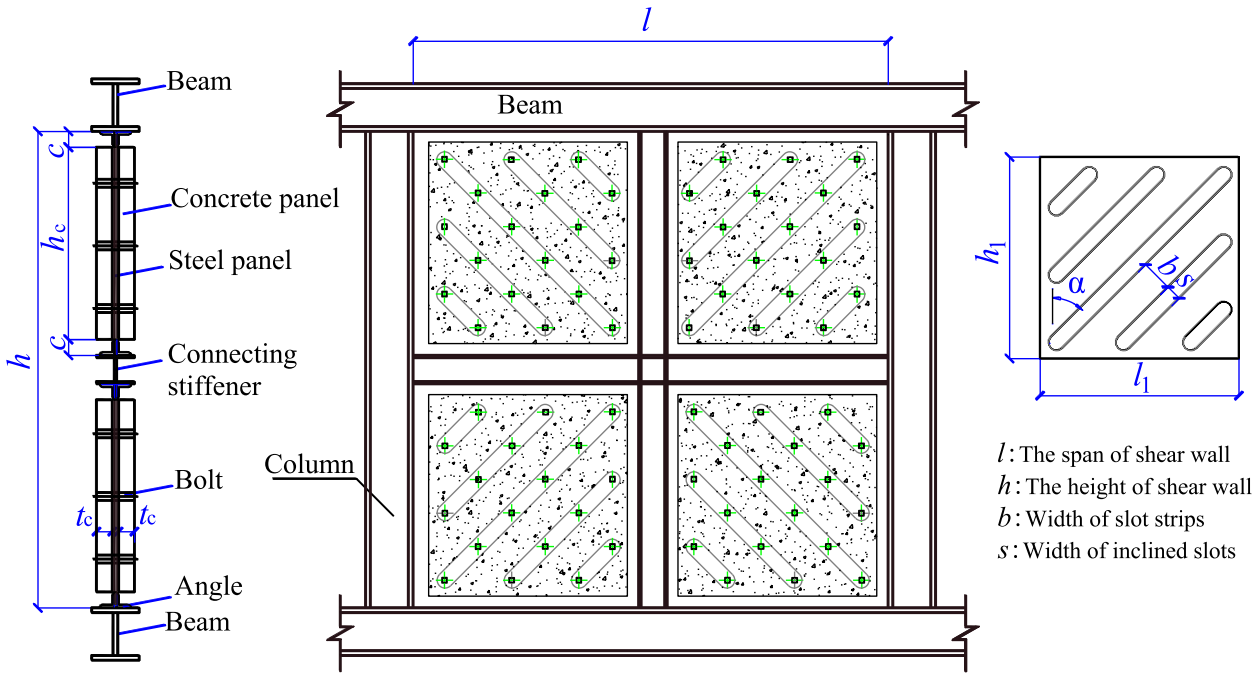

Fig. 2 Configuration of the MSPSW

and controlled quality of the embedded steel plate with inclined slots enable uniform industrial production that is easy to process and transport.

FE model of the MSPSW

The FE software ABAQUS was used to build the FE models of MSPSW. The MSPSW FE models have a span of 1500 mm and a height of 1500 mm. To simplify the calculation and focus on the behavior of the slotted SPSW and MSPSW, their beams and columns are hinged.

In order to achieve the purpose of inner slotted steel plate yielding before the frame, the steel strength of the frame and T&L connecting stiffener is chosen Q345, and the cross-sectional dimensions of the beams and columns are 300 mm×150 mm×18 mm×20 mm.The dimension of the connecting stiffeners is shown in the specific analysis model. The steel strength of the inner slotted steel plate is Q235, and the angle of inclined slots is 45° or 135°.The slots of the adjacent steel plate are symmetrically arranged. The concrete panel is made of C30 concrete and is equipped with double-layer bidirectional distributed steel bars (HPB300, diameter 8 mm, spacing 100 mm).

When building the MSPSW FE modeling, B31 beam element is used for the beams and columns, S4R shell element for steel plates, and C3D8R solid element for concrete panels. The beams and columns are connected together by coupling constraints, and U1, U2 and U3 degrees of freedom are constrained to achieve the simply connection of beams and columns. It is assumed that there is no damage in the connection. "Tie" restrained connection is adopted between steel plate and surrounding components. "Surface-to-surface" contact is the sort of contact between the slotted steel plate and concrete panels. The contact type is "hard" contact, that is, only the normal stress is transmitted, and the friction coefficient is 0.005. Bolting of concrete on both sides of the steel plate is modelled using the "Coupling" constraints to constrain the out-of-plane degrees of freedom. T3D2 truss element is adopted for steel bar, and "Embedded" connection method is adopted to embed into concrete panel to form reinforced concrete panel. In this study, the thickness of each side of the steel plate is increased by 20 mm to simulate the function of a fishplate. The distance between the end of the inclined slots and the edge of the steel plate is set at 125 mm. When meshing, the concrete solid elements are divided into 40, and the remaining component elements are divided into 20. The FE model is shown in Fig. 3. The finite element modeling approach of slotted SPSW remains the same as that of MSPSW, except that there is no T&L connecting stiffener.

The bilinear curve is used to describe the stress–strain relationship as the steel material (Fig. 4a). The Young's modulus Ee is 200 GPa, the Poisson's ratio of steel ν is 0.3, and Young's modulus of the strengthening section is 0.02 Ee. for Q345 steel, the yield stress fy is 345 MPa. And for Q235 steel, the yield stress fy is 235 MPa, The ultimate stress fu is 1.5 times of the yield stress. The concrete

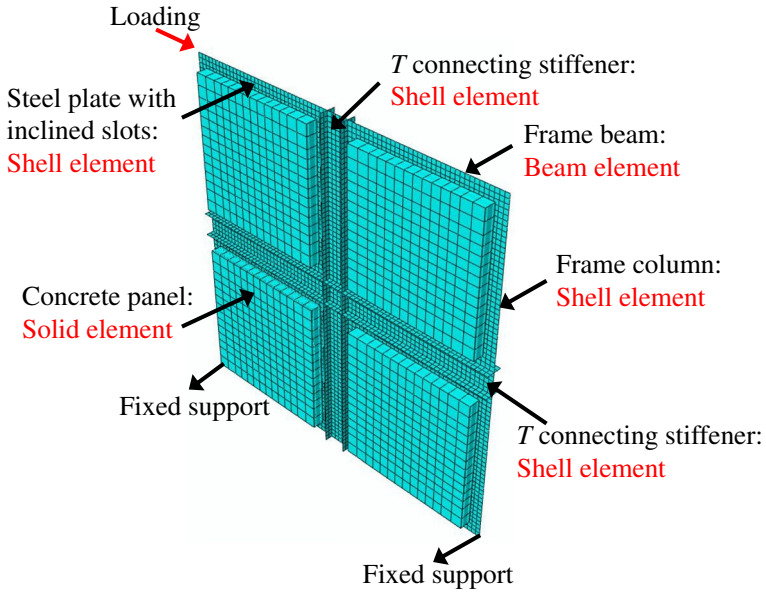

Fig. 3 Finite element model

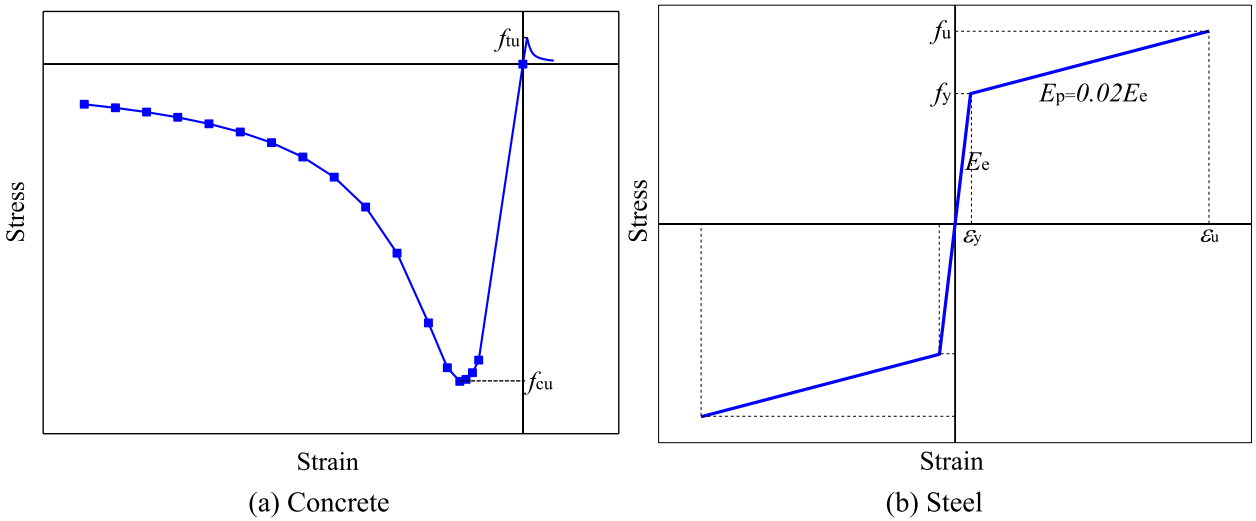

Fig. 4 Stress–strain curves for the concrete and steel material

damage plastic model (CDP model) is used to simulate the concrete behavior and the constitutive relationship recommended by the Concrete Structure Design Specification (GB50010-2010) is adopted as the concrete material (Fig. 4b).

The model's eigenvalue buckling analysis is used to determine the structure's most likely buckling deformation, which is taken as the structure's initial defect according to a specific amplitude. The defect amplitude is 1 mm. The loading is then controlled using the top beam end displacement, with a maximum drift ratio of 2%.

The FE model was confirmed by composite steel plate shear wall in Guo's experiment [25]. Figure 5 shows the hysteresis curves for the quasi-static cyclic loading situations. It is evident that the shear resistance and the experimental result coincide well. Therefore, the modeling methodology is confirmed.

Seismic behavior of the MSPSW

In the subsections that follow in this paper, a number of different parameter models are designed to consider the influence of slots width, slots spacing, steel

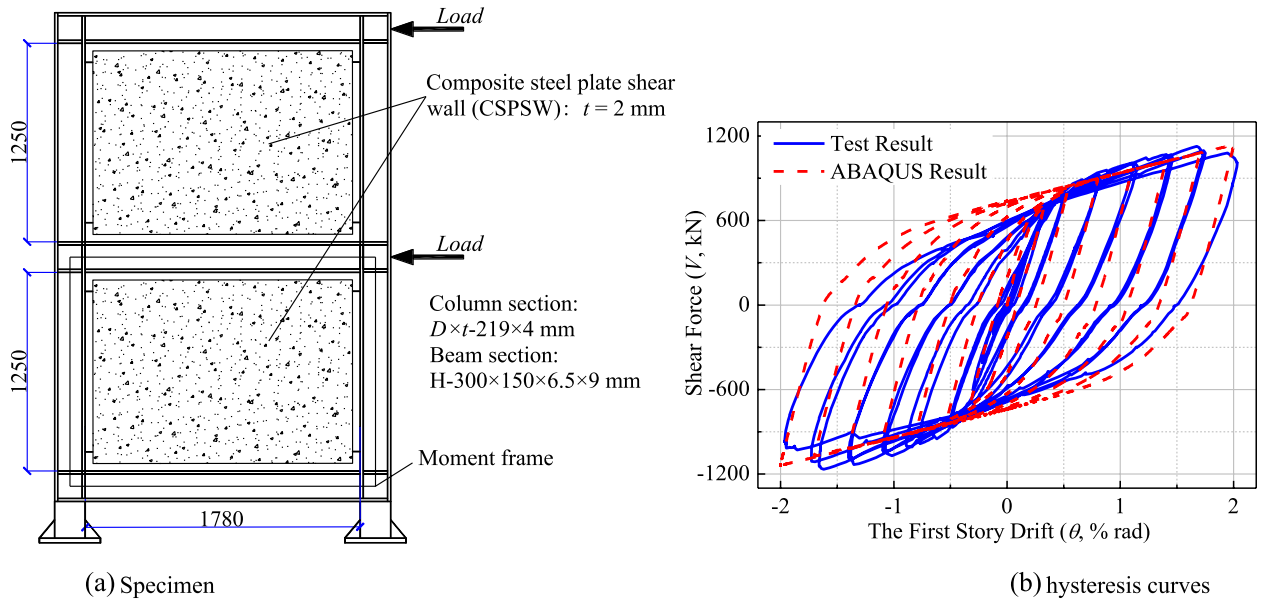

Fig. 5 Comparison of hysteresis curves under cyclic loads

plate thickness, and cross-sectional dimensions of T&L connecting stiffener on the MSPSW. The relationship between drift ratio and horizontal load was investigated. Table 1 depicts the specific parameters of the models.

General behavior of a typical MSPSW

To analyze the overall behavior under the horizontal force, a typical MSPSW is chosen. The cross-sectional dimension of the T&L connecting stiffener of the shear wall is 100×68×4.5×7.6, the spacing between the slots is 200 mm, the width of the slots is 15 mm, and the thickness of the slotted steel plate is 5 mm. Figure 6 depicts the relationship between horizontal load and drift ratio.

When the horizontal load is small, the model's initial tangential stiffness is 319 kN/m. The embedded steel plate is in the elastic state. The first noticeable decrease in tangent stiffness is observed with an increase in load and corresponds to point A. The Mises stress distribution of the MSPSW corresponding to point A is shown in Fig. 7a. Currently, the local stress in a few places on the steel plate is greater than the steel's yield stress. As the horizontal stress increases, the slotted steel plate

Table 1 Component parameters (unit: mm)

Inner steel plates					Connecting stiffener dimension
Models	Thickness	Dimensions	Width of inclined slots	Width of slot strips	
SPSW-0	5	1500×1500	50	200	/
MSPSW-1	5	700×700	25	100	100×68×4.5×7.6
MSPSW-2	5	700×700	25	150	100×68×4.5×7.6
MSPSW-3	5	700×700	25	200	100×68×4.5×7.6
MSPSW-4	5	700×700	15	200	100×68×4.5×7.6
MSPSW-5	5	700×700	50	200	100×68×4.5×7.6
MSPSW-6	5	680×680	50	200	140×80×5.5×9.1
MSPSW-7	5	670×670	50	200	160×88×6.0×9.9
MSPSW-8	5	650×650	50	200	200×100×7.0×11.4
MSPSW-9	4	700×700	15	200	100×68×4.5×7.6
MSPSW-10	3	700×700	15	200	100×68×4.5×7.6

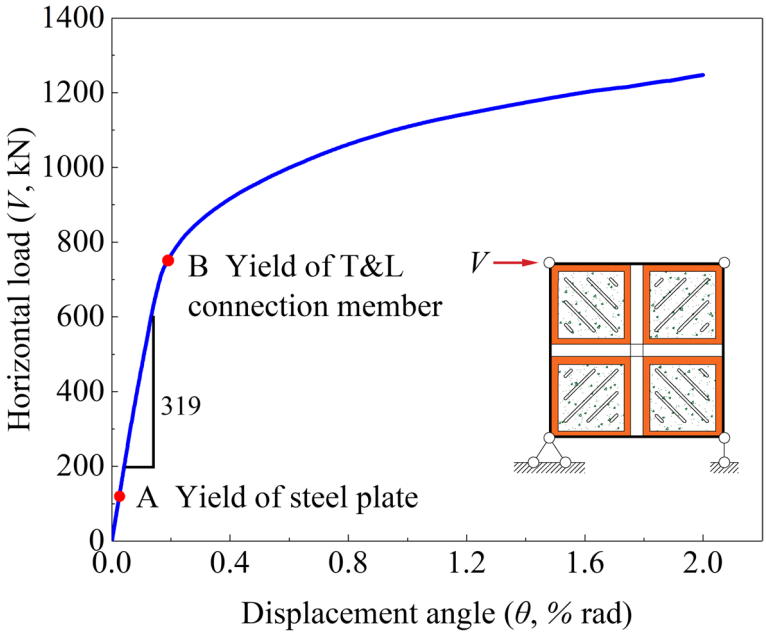

Fig. 6 Horizontal load-drift ratio curve of the MSPSW

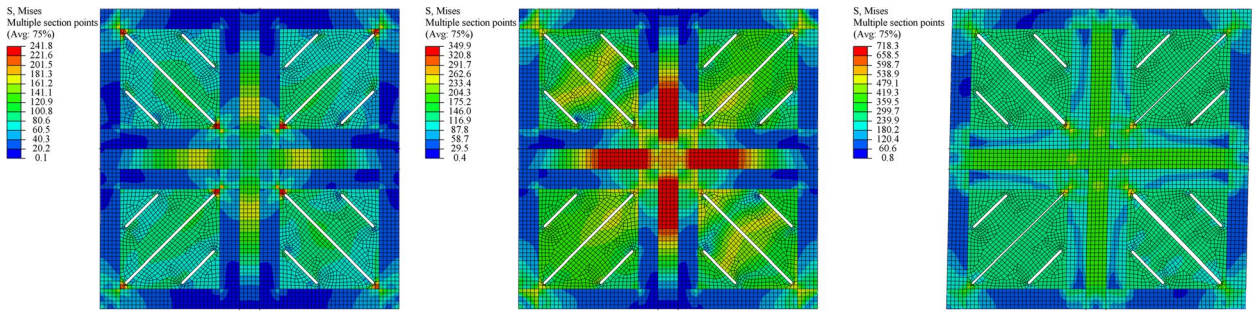

(a) Point A (b) Point B (c) Drift ratio of 2.0%

Fig. 7 Mises stress distribution of the MSPSW

enters the stage of elastic–plastic deformation, and point B corresponds to the second clearly observed decrease in tangent stiffness. From the Mises stress distribution in Fig. 7b, the slotted steel plates have yielded in full section, and the T&L connecting stiffener also enter the yield stage. As the load increases further, the entire component enters the post-yield strengthening phase, as shown in Fig. 7c. At this time, the steel plate and T&L connecting stiffener are in the stage of plastic strengthening, and the bearing capacity is further improved.

Influence of T&L connecting stiffener

In order to investigate the effect of dimensions of T&L connecting stiffener on the bearing capacity of MSPSW,the models of SPSW-0, MSPSW-5, MSPSW-6, MSPSW-7 and MSPSW-8 in Table 1 are selected and analyzed. It should be noted that the other parameters in the model are constant, the only difference is cross-section of the connecting stiffener. Figure 8 illustrates the comparison of the horizontal load-drift ratio curves for various T&L connecting stiffener dimensions.

The yield load capacity of the members is 704 kN, 830 kN, 878 kN, 996 kN, and 527 kN, respectively, when the web sizes of T&L connecting stiffeners are 100 mm, 140 mm, 160 mm, and 200 mm, and when T&L connecting stiffeners are not used. The stiffnesses are 295 kN/mm, 317 kN/mm, 329 kN/mm, 353 kN/mm, and 163 kN/mm, respectively. It is evident that steel plate shear walls with T&L connecting stiffeners have much higher initial elastic stiffness and bearing

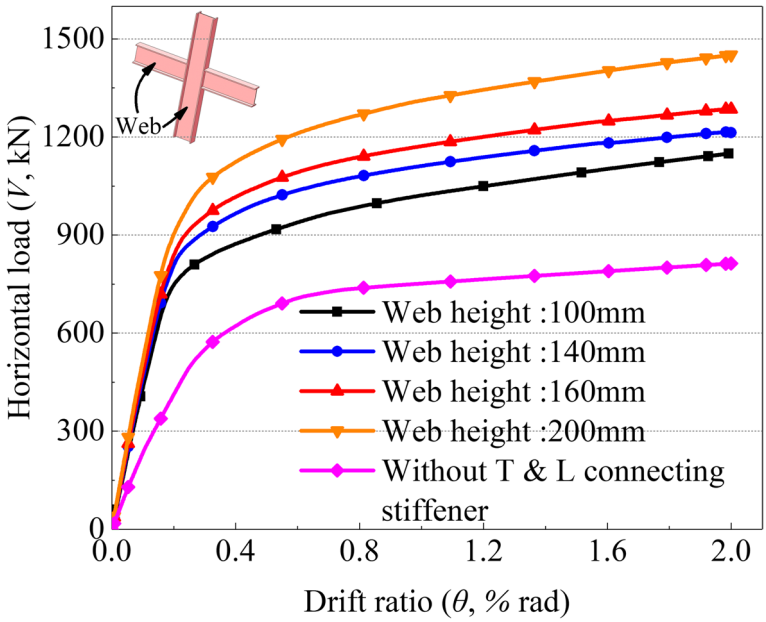

Fig. 8 Horizontal load—drift ratio curves of the MSPSW with different connecting stiffener

capacity than those without them. Furthermore, the overall mechanical properties of the MSPSW are significantly strengthened with the increase in the cross-section dimension of the T&L connecting stiffeners. The strength and overall stiffness of MSPSW have increased to some extent since the addition of the T&L connecting stiffeners.

Influence of the width of inclined slots and strips

To study the effect of slots width on mechanical properties of the MSPSWs, the models of MSPSW-3, MSPSW-4 and MSPSW-5 in Table 1 are selected and analyzed. Other parameters in the models remain consistent. The comparison of the horizontal load-drift curves with different inclined slots width are shown

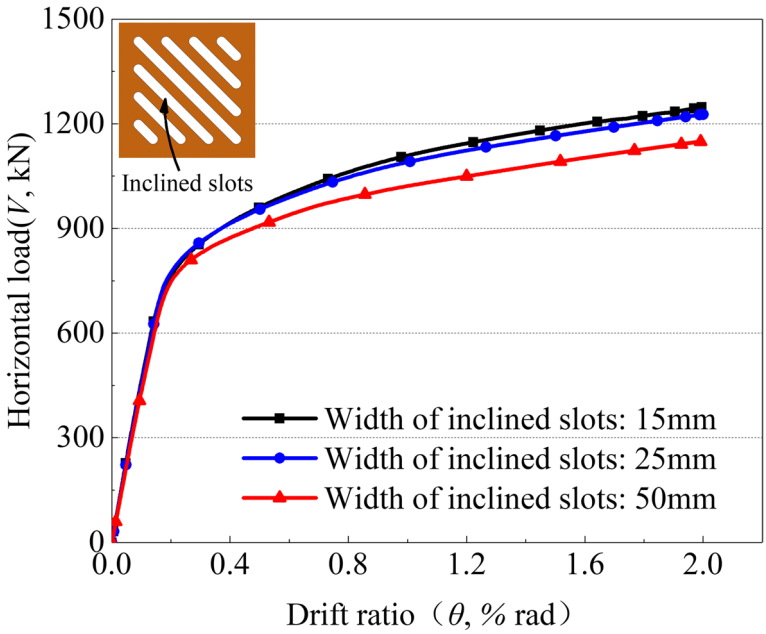

Fig. 9 Horizontal load—drift ratio curves of the MSPSW with different inclined slots

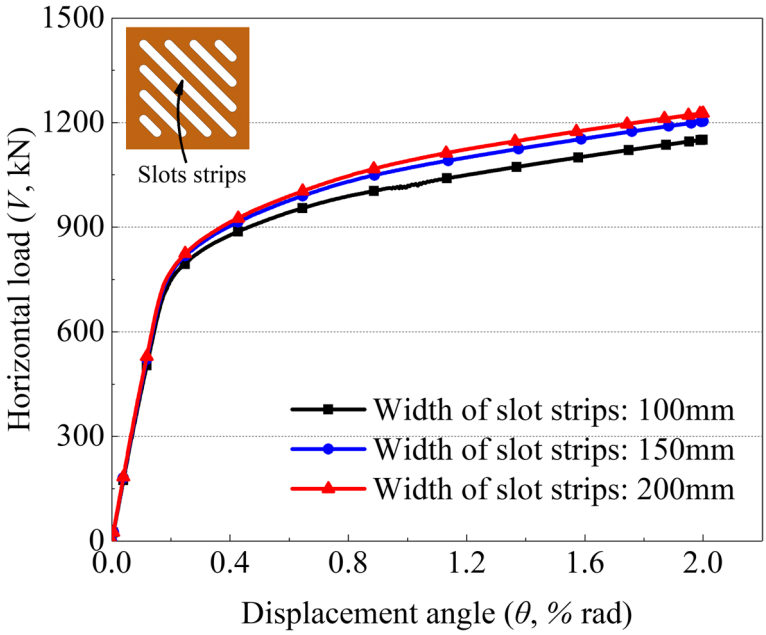

Fig. 10 Horizontal load—drift ratio curves of the MSPSW with different slot strips

in Fig. 9. As can be observed, each curve has essentially the same features. The shear wall initially has a high initial stiffness and is in the elastic stage.When a part of the slot strips and the T&L connecting stiffener enter the yield stage, the tangent stiffness changes obviously, and as they move into the yield stage, the component's bearing capacity gradually increases. The MSPSW's elastic stiffness and yield bearing capacity increase as the width of the inclined slots is reduced. When the width of corresponding inclined slot is 15 mm, 25 mm and 50 mm, the initial tangent stiffness is 319kN/mm, 313 kN/mm and 295kN/mm respectively, and the yield bearing capacity is 762kN, 735kN and 704kN respectively.

It is established via the use of the MSPSW-1, MSPSW-2, and MSPSW-3 models that the width of the slot strips has an impact on the bearing capacity of MSPSW. Note that the models have the same inclined slot width of 25 mm. Figure 10 shows the relationship curve of horizontal load and drift ratio of MSPSW under different width of slot strips. It can be seen from the figure that when the width of the slot strips corresponding to models are 100 mm, 150 mm, and 200 mm, the yield bearing capacity is 707kN, 718kN, and 735kN, respectively, and the initial tangential stiffness is 296kN/mm, 307kN/mm, 312kN/mm respectively. It can be found that with the increasing of the width of the slot strips, the capacity of the MSPSW increases.

Influence of the width of steel plate

To study the effect of steel plate thickness on mechanical properties of the MSPSWs, the models of MSPSW-4, MSPSW-9 and MSPSW-10 in Table 1 are selected and analyzed. The horizontal load-drift ratio curve of the MSPSW with different slotted steel plate thicknesses is depicted in Fig. 11. It is obvious that as steel plate thickness has risen, MSPSW performance has significantly improved. The yield bearing capacity of corresponding steel plates with thicknesses of 3 mm, 4 mm, and 5 mm is 536 kN, 680 kN, and 762 kN, respectively. Initial tangential stiffness is 224 kN/mm, 274 kN/mm, and 319 kN/mm, respectively.

The requirements of the out-of-plane restraint members

To make sure that the slotted strips can appropriately participate in the forces under the load of MSPSW, the precast concrete panels are employed as the out-of-plane restraint member for the slotted steel plates. The primary determining element in how efficiently the sloted steel plate is restrained is the thickness of the concrete panel (Tc). In Fig. 12, the hysteresis curves for concrete slabs that are 50 mm, 100 mm, and 200 mm thick are compared. Keep in mind that the steel plate is 1500 mm × 1500 mm in size, the inclined slots are 50 mm wide, and they are 200 mm apart.The hysteresis curve exhibits a significant pinch phenomenon at concrete panel thicknesses of 50 mm.This reduction in bearing

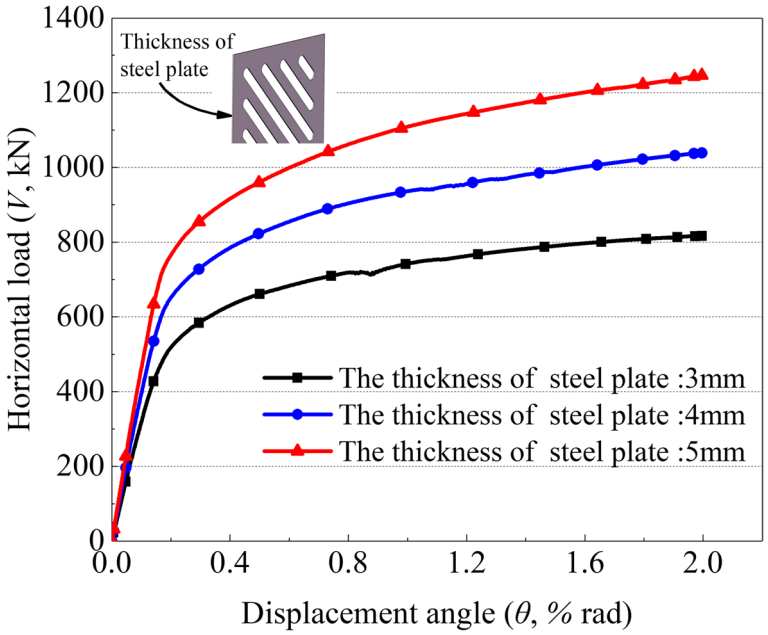

Fig. 11 Horizontal load—drift ratio curves of the MSPSW with different steel plate thickness

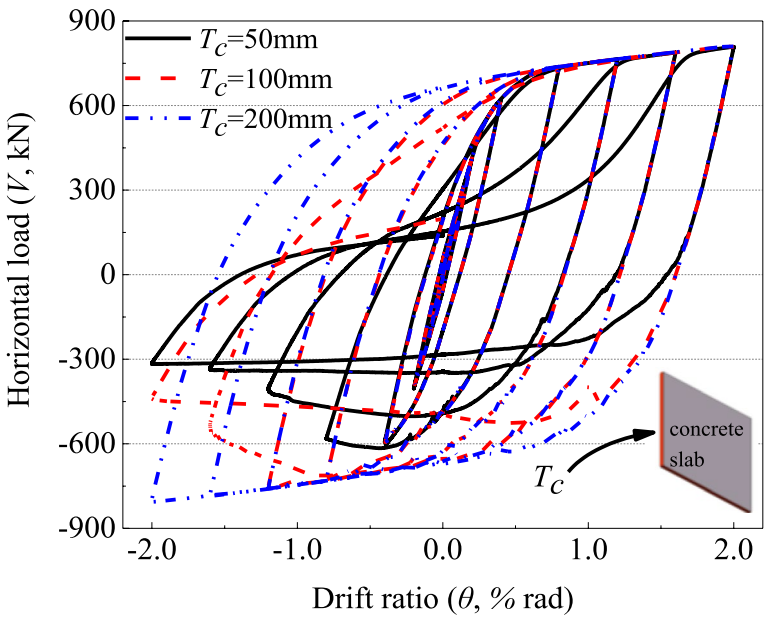

Fig. 12 Comparison of hysteresis curves for different concrete panel thickness

capacity is due to insufficient out-of-plane constraints provided by concrete panel. The pinching phenomenon appearing in the hysteresis curve is improved as the concrete panel thickness increased. When the concrete panel thickness is chosen to be 200 mm, sufficient out-of-plane stiffness can be provided. At this time, the hysteresis curve is plump and the energy consumption is stable.

In Fig. 13, two finds of steel shear walls' hysteresis curves—one with and one without T&L connecting stiffeners—are contrasted. The remaining parameters of the two types of shear walls remain the same, and the thickness of the concrete panels is 50 mm. It has been determined that a concrete panel with a thickness of 50 mm can offer enough out-of-plane constraints for SPSWs with

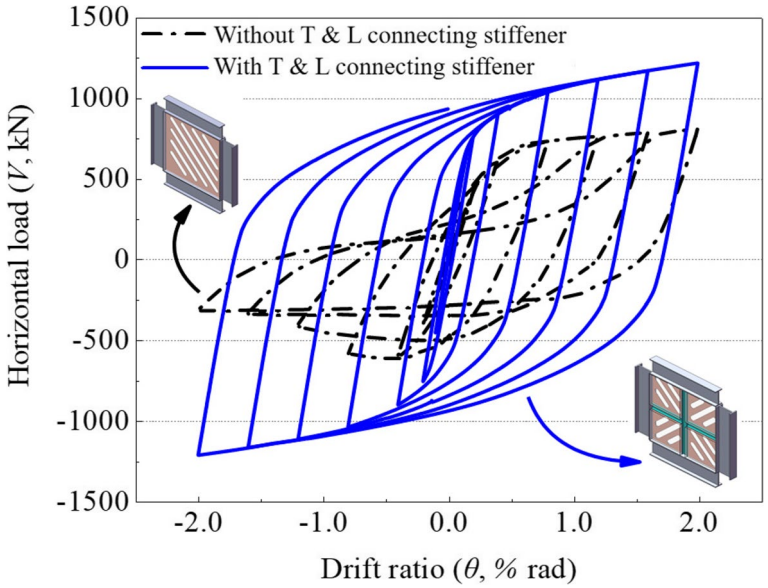

Fig. 13 Comparison of hysteresis curves of two types of shear walls (Tc = 50 mm)

T&L connection member, whereas a concrete panel with a comparatively higher thickness should be used for SPSWs without a T&L connection member. As can be observed, installing T&L connecting stiffeners allows for a reduction in the need for inner steel plate out-of-plane restraint.

The steel plate shear wall's hysteresis loop area, which measures the wall's capacity to dissipate energy, is another crucial parameter. Figure 14 shows the area surrounded by hysteretic loop of shear walls with different thickness of concrete panel without T&L connecting stiffener, and the comparison of the area surrounded by hysteretic loop of shear walls with 50 mm thickness of concrete panel when T&L connecting stiffener are set. As can be observed, the hysteresis loop's surrounding area is rather tiny during the initial loading phase since the shear wall is essentially in the elastic phase. For the SPSW without T&L connecting stiffener,when the drift ratio between layers is

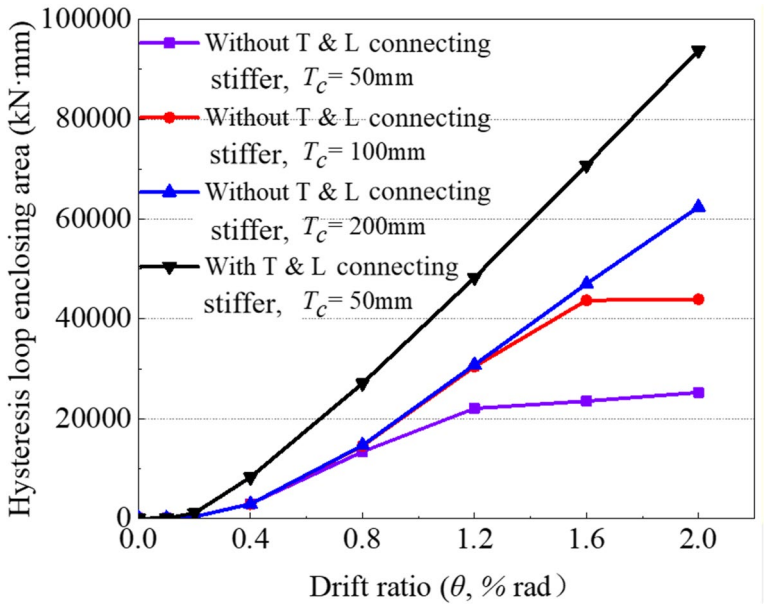

Fig. 14 Comparison of the area enclosed by hysteresis loops

less than 0.8%, the area surrounded by hysteretic loop is approximately the same; then, under the same drift ratio between layers, the region surrounded by the hysteretic loop gets bigger as the concrete panel's thickness grows. Additionally, as the T&L connecting stiffener are offered to somewhat increase the overall rigidity of the MSPSW, the capacity for dissipating energy is improved. The region surrounded by the hysteretic loop of MSPSW is bigger than that steel plate shear walls without the T&L connecting stiffener when the drift ratios are equal.

A comparison of the energy dissipation coefficient for the two varieties of slotted SPSWs is shown in Fig. 15. As can be observed, the energy dissipation coefficient grows slowly during the initial loading phase because the shear wall is in an elastic state, but afterwards it increases quickly. When the drift ratio θ is 1.2% and the shear wall has concrete panels that are 50 mm thick, the energy dissipation coefficient of the wall drops without the T&L connecting stiffener. This results from inadequate concrete panels restraint capacity during loading. Similar to this, for concrete panels with a thickness of 100 mm, the energy dissipation coefficient starts to drop when the drift ratio is 1.6%. There is no reduction in the energy dissipation factor for slotted SPSW with a 200 mm thick concrete panels. Furthermore, the figure shows that the energy dissipation coefficient of MSPSW is greater than that of the SPSW without T&L connection stiffener for the same drift ratio, and the energy dissipation coefficient of MSPSW does not decrease. The ability to dissipate energy has improved once the T&L connecting stiffener was set.

Development process of internal forces in the boundary members

The appropriate choice of the boundary column has a significant impact on the mechanical characteristics of the shear wall. To compare the internal force generation process, the ordinary slotted SPSW and MSPSW are chosen. The two different types of shear walls have slot strips that are 200 mm wide, slots that are 50 mm wide, and steel plates that are 5 mm thick.

Internal force analysis of the ordinary slotted SPSW

Axial force in the column

Under a horizontal load to the right, Fig. 16 shows the pattern of development of the axial force distribution in the left and right columns with increasing drift ratio. As can be observed, the axial force increases slowly after the shear wall enters the plastic stage. The columns on both sides are in different stress states under external loads. Specifically, the left column's axial force develops from positive to negative values from the bottom to the top of the column when external load and the inclined strip are acting together. For both sides of the frame columns, the greatest axial force appears at the bottom. The maximum axial force for the left column is -645 kN and -1170 kN for the right column. It is worth noting that the axial force around the middle of the left column is 0,

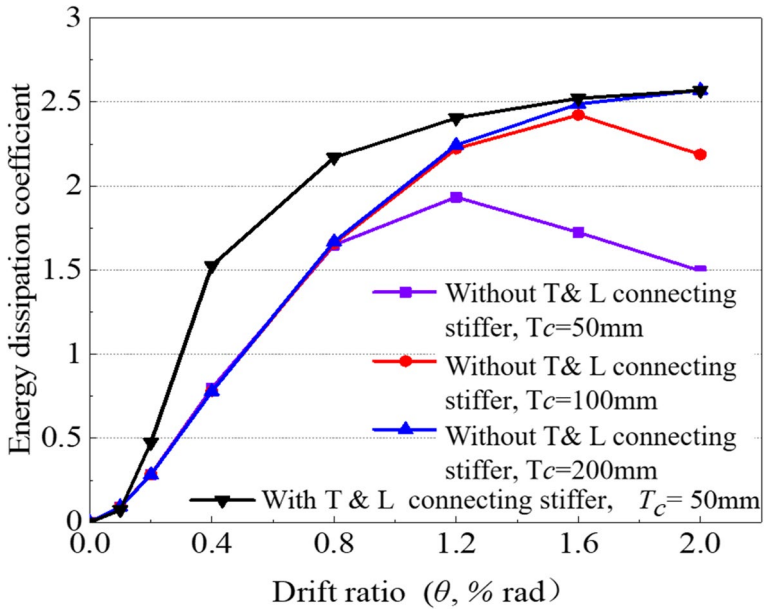

Fig. 15 Comparison of the energy dissipation coefficient

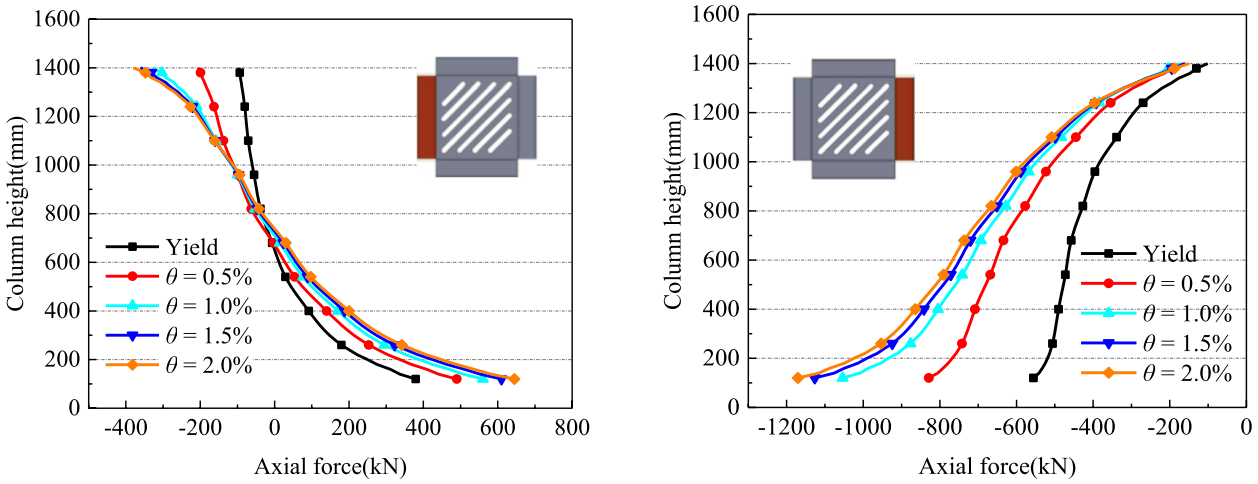

Fig. 16 The development of axial force in columns of the ordinary slotted SPSW

indicating that its stress state has changed from tension to compression.

Shear force in the column

Figure 17 shows the evolution of shear force distribution throughout the left and right columns' heights with the increasing drift ratio under the right horizontal load. As can be seen, the shear force is distributed fairly linearly along the height. For the left column, the shear force develops from negative to positive values from the bottom to the top, and the maximum shear force appears at the top of the column at 361 kN. The shear distribution patterns of the right column is close to antisymmetric with the left column, and the maximum shear force appears at the bottom of the column, which is + 386 kN.

Bending moment in the column

Figure 18 illustrates the development of bending moment distribution along the left and right columns' heights as the drift ratio increases. It can be seen that the bending moment distribution of the columns on both sides is similar to that of the simply supported beam under uniform load. Its maximum bending moment appears in the middle position, and the bending moment values on both sides are zero. The left column's maximum bending

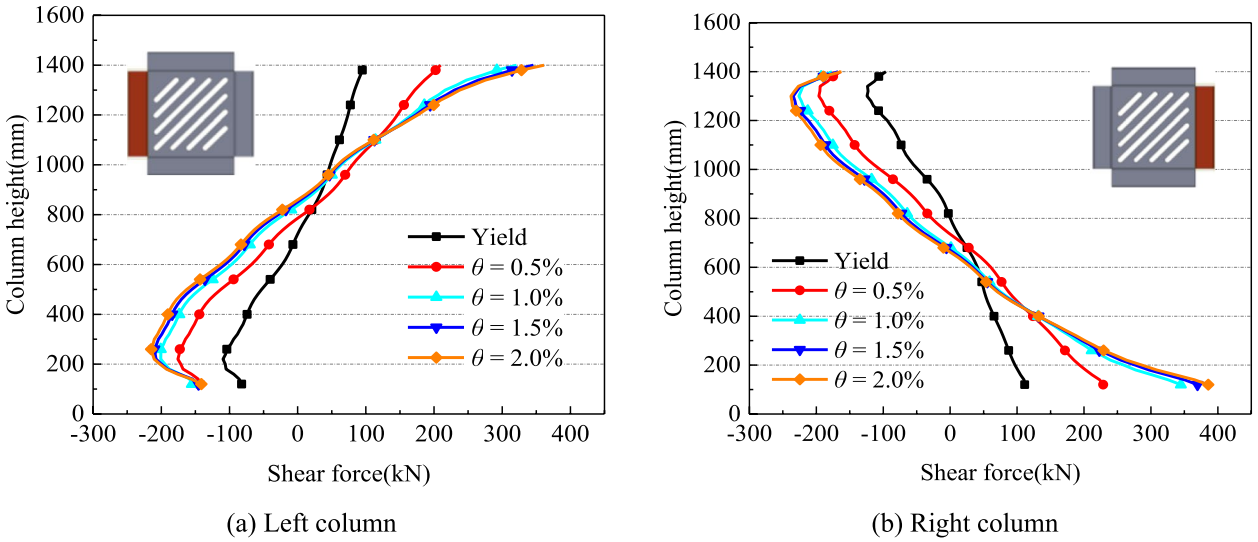

Fig. 17 The development of shear force in columns of the ordinary slotted SPSW

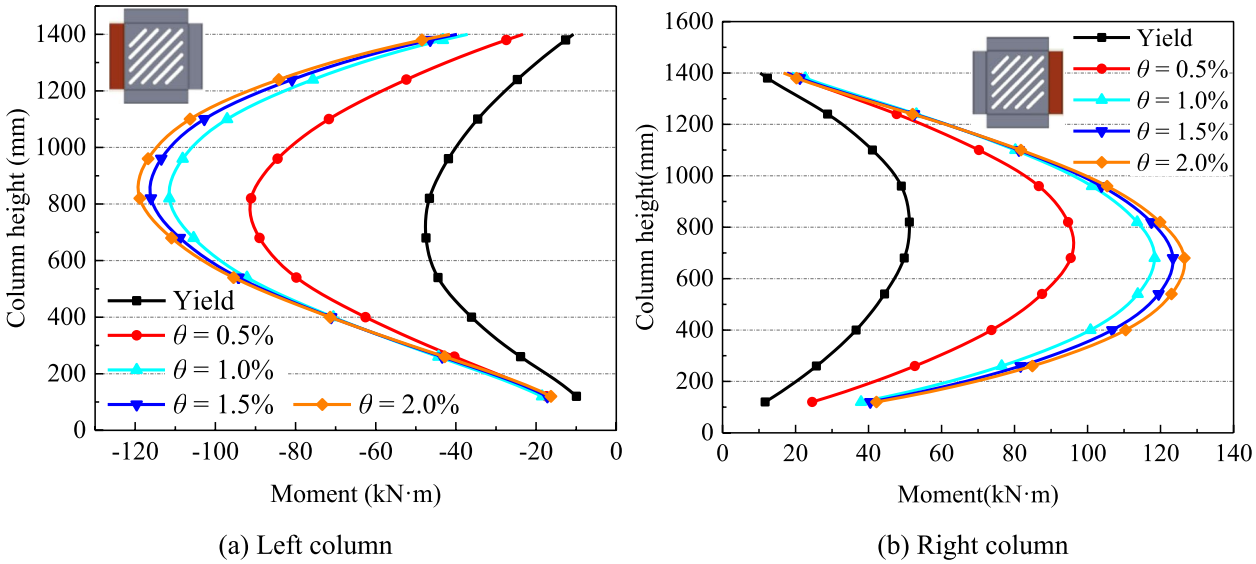

(a) Left column (b) Right column

Fig. 18 The development of bending moment in columns of the ordinary slotted SPSW

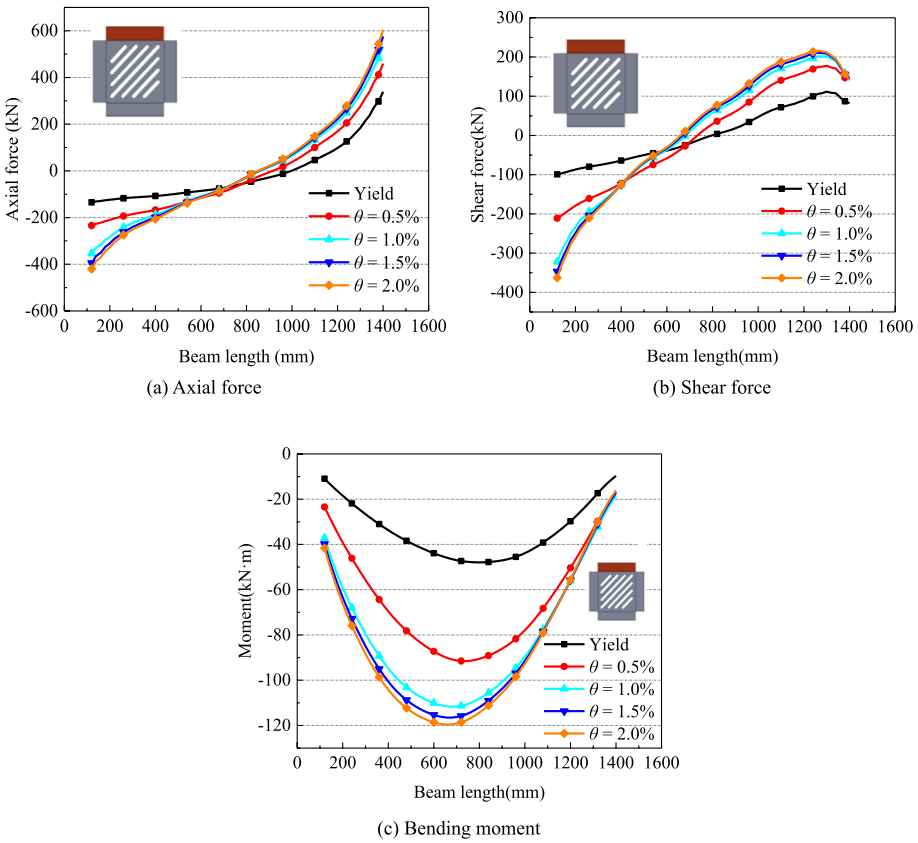

(a) Axial force (b) Shear force

(c) Bending moment

Fig. 19 The development of internal force in beam of the ordinary slotted SPSW

moment is -119kN·m, while the right column's maximum bending moment is + 127 kN·m. The left and right columns' bending moment distribution patterns are roughly anti-symmetric.

Internal forces in the beam

Figure 19 illustrates the pattern of internal force development along the top beam as the drift ratio rises. As shown in Fig. 19a, after the beam enters the yielding phase, the axial force gradually increases. The distribution is roughly linear. The stress state shifts from compression to tension from left to right, moving from negative to positive values. The right end beam's maximum axial force, which is 604kN, is somewhat higher than that of the left end. According to Fig. 19b, the shear force distribution in a beam is roughly linear over the length of the beam, with a maximum shear force of -363kN at the left end and a slightly greater shear force at the left end. When a vertical uniform load is applied, the bending moment distribution resembles that of a beam that is simply supported. In the mid span position, there is a -196 kN·m maximum bending moment.

Internal force analysis of the proposed MSPSW

Since the existence of T&L connections, mechanical properties of the MSPSW can be improved, and the demand of boundary members can be reduced.

Axial force in the column

The evolution of axial force in MSPSW columns is depicted in Fig. 19. It can be observed that the axial force distribution of the left and right columns is symmetrical. Their axial forces increase with height from top to bottom, and the maximum axial force appears at the bttom of the column. For the left column, its maximum axial force is 1072kN and for the right column it is -1040kN. Additionally, there is no noticeable rise in the axial force at the middle of the left and right columns. The axial forces of the columns are slightly decreased as compared to the SPSW without the T&L connecting stiffener Fig. 20.

Shear force in the column

The development of shear force in MSPSW columns is depicted in Fig. 21. Due to the addition of the T&L connecting stiffener, the MSPSW's shear distribution pattern differs significantly from that of the ordinary slotted SPSW. The shear force are negative at both ends of the columns and increase gradually toward the middle of the column. The maximum shear force occurs at the middle of the column. The steel plates with inclined slots in each grids respectively exert a uniform force on the boundary column. The boundary column (beam) is divided into upper and lower (left and right) parts by T&L connecting stiffener. Comparing the maximum shear force of the MSPSW to the ordinary slotted SPSW, a reduction of about 50% is observed.. In the design of column section, the smaller dimension of column can meet the demand of shear capacity.

Bending moment in the column

The development of bending moment in MSPSW columns is depicted in Fig. 22. Since the setting of connecting stiffener, the boundary column is divided into the upper part and the lower part. The left and right columns' axial force distribution patterns can be shown to be similar. The maximal column bending moment occurs near the middle

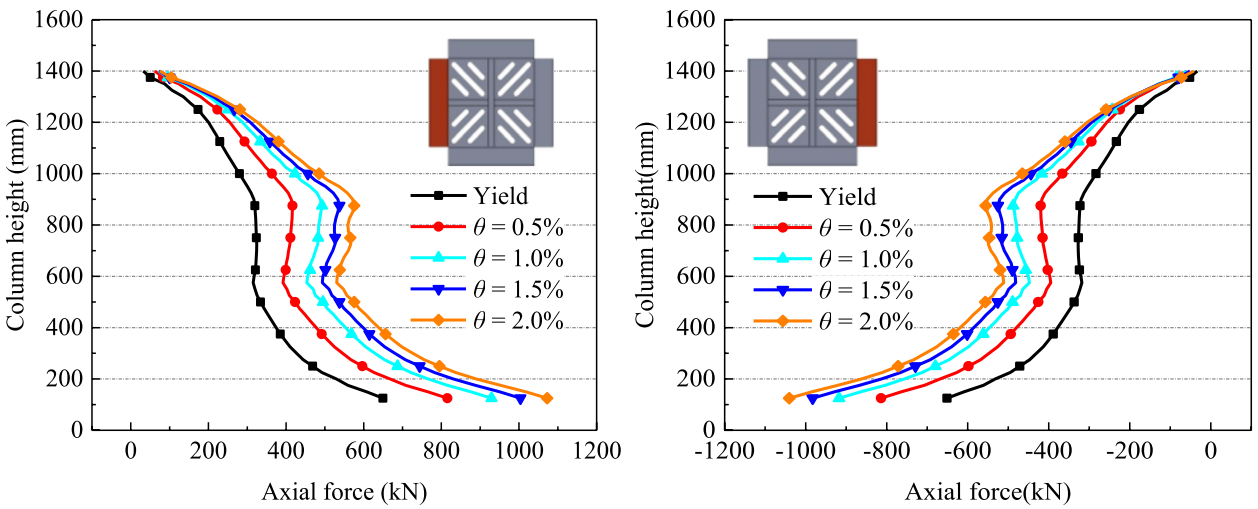

(a) Left column (b) Right column

Fig. 20 The development of axial force in columns of the MSPSW

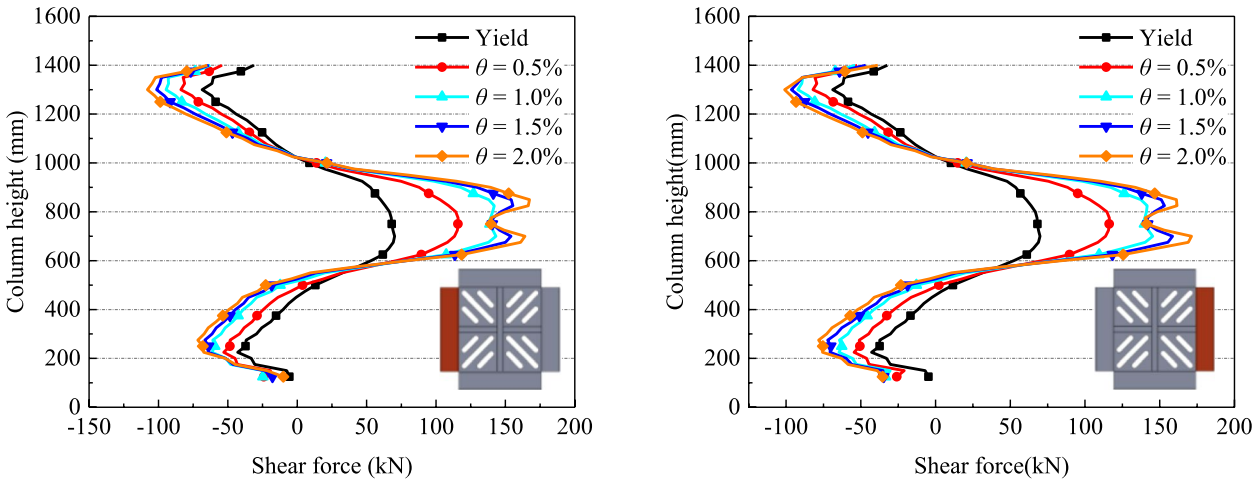

(a) Left column (b) Right column

Fig. 21 The development of shear force in columns of the MSPSW

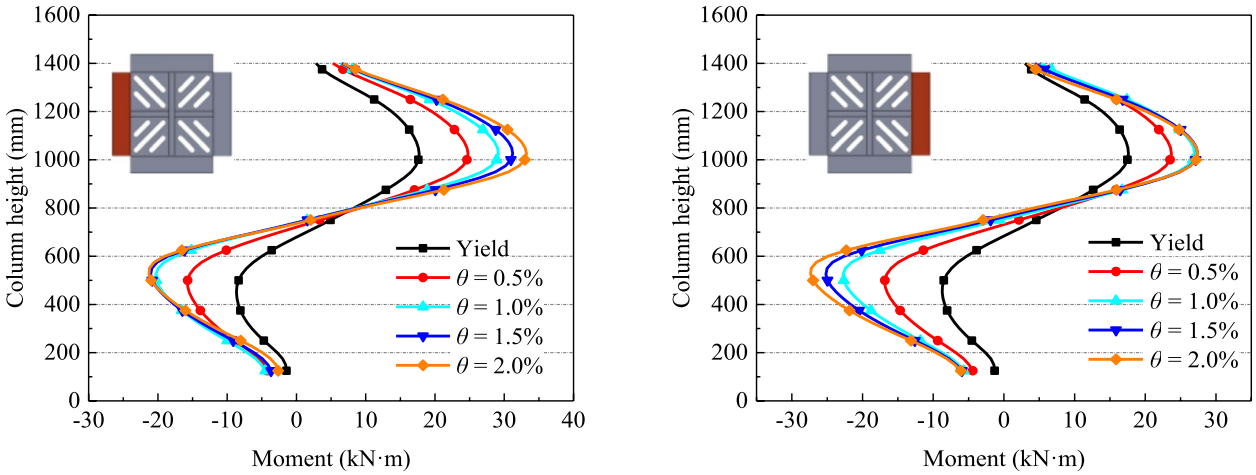

(a) Left column (b) Right column

Fig. 22 The development of bending moment in columns of the MSPSW

of the upper and lower parts of the column.The moment distribution of the upper and lower parts of the frame column is similar to that of the simply supported beam under uniform load. The bending moment is about 0 for the column's end and its middle point. For the left column, the maximum positive bending moment is + 33 kN·m and the maximum negative bending moment is -21 kN·m. For the right column, it is + 27 kN·m and -27 kN·m, respectively. Compared with the ordinary slotted SPSW, the maximum moment in the columns of MSPSW is significantly reduced, which is only about a quarter of the original value. When designing the column section according to the bending moment, the demand for the section dimension of the frame column is reduced significantly.

Internal forces in the beam

Figure 23 depicts how internal forces evolved along the top beam. As depicted in Fig. 23a, the axial force distribution on the beam is roughly linear, with a slight overshoot occurring in the center of the beam span. The axial force develops from negative to positive value from left to right, and the stress in the beam changes from compression to tension. According to Fig. 23b, the beam's end and the span have the highest shear values. The shear force in the beam changes from positive at the left end to negative in the middle of the span, and then it changes back to positive at the right end. The beam has a maximum positive shear force of + 91 kN and a maximum negative value of -161 kN. The bending moment distribution

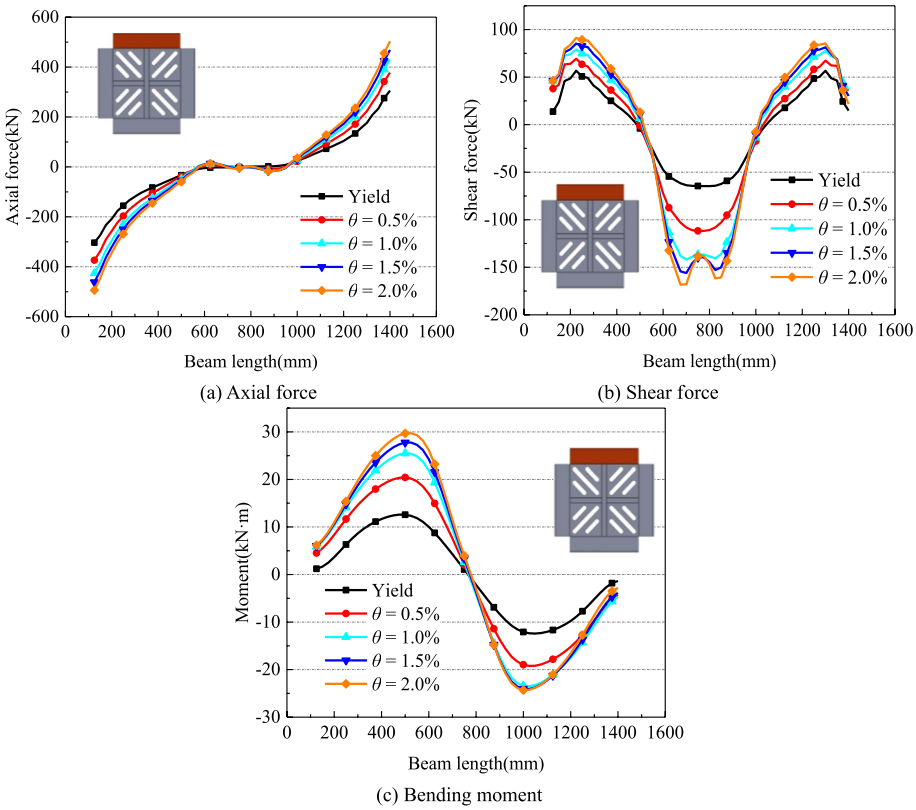

Fig. 23 The development of internal force in beam of the MSPSW

is similar to frame columns as shown in Fig. 23c. The bending moment of the left part of the beam is positive, and the beam is affected by the upward distributed force similarly. The left half of the beam's mid-span location is where the highest bending moment, which has a maximum positive moment of + 30 kN·m. The moment in the right half of the beam is negative, and the beam is similarly affected by the downward distributed force. The right half of the beam's maximum bending moment is approximately midway through its span, and its maximum negative bending moment is—24 kN·m. Compared with the ordinary slotted SPSW, the stress on the frame beam of the MSPSW is reduced, which reduces the demand for the frame beam section.

Theoretical design method of internal forces

Theoretically, the maximum internal force of the boundary columns of the ordinary slotted SPSW in hinged frame under the horizontal load is equal to the following, according to reference [26].

Maximum axial force:

$$N_{max} = 0.75\ \alpha_n \cdot f_y \cdot l \cdot t \tag{1}$$

Maximum shear force:

$$V_{max} = 0.25\ \alpha_n \cdot f_y \cdot l \cdot t \tag{2}$$

Maximum bending moment:

$$M_{max} = \frac{1}{6}\alpha_n \cdot f_y \cdot t \cdot h^2 \tag{3}$$

Where $\alpha_n = 1\text{-}0.71 \times n \times s / l$ is the reduction of bearing capacity by inclined slots, n is the number of inclined slots, s is the width of the inclined slots, l is the span of steel plate shear wall, f_y is the yield strength of the inner steel plate and t is the thickness of the inner steel plate.

The numerical analysis comparison between the MSPSW and the ordinary slotted SPSW with the same dimension shows that the maximum axial force of the MSPSW is not significantly different from that in the ordinary slotted SPSW, while the shear force and bending moment of the MSPSW are reduced by about half and about three-quarters, respectively. The maximum internal force can be calculated as:

Maximum axial force:

$$N_{max}^{ms} = 0.75 \cdot \alpha_n \cdot f_y \cdot l \cdot t \tag{4}$$

Maximum shear force:

$$V_{max}^{ms} = \frac{1}{8.}\alpha_n \cdot f_y \cdot l \cdot t \quad (5)$$

Maximum bending moment:

$$M_{max}^{ms} = \frac{1}{64.}\alpha_n \cdot f_y \cdot t \cdot h^2 \quad (6)$$

Based on the results of FE analysis, the control internal forces of the beam and column sections of MSPSW are almost the same. The maximum internal force on the beam can roughly follow the above formula. The parameters n = 9, s = 500 mm, l = 1500 mm, $f_y = 235$ N/mm^2, t = 5 mm, h = 1500 mm are brought into the equations, and the maximum axial force in column of the MSPSW can be calculated $N_{max}^{ms} = 1031$kN, maximum shear force $V_{max}^{ms} = 171$kN, and maximum bending moment $M_{max}^{ms} = 32\text{kN} \bullet \text{m}$. This is slightly less than the results of the finite element calculation, and the main cause of its error is because the theoretical calculation did not account for the effect of steel plate strengthening.

Conclusion

In this paper, a new type of the MSPSW is provided. By setting T&L connecting stiffener, the internal space of the frame is divided into several small grids, and small-sized slotted steel plates are set in the grids. Mechanical properties under the horizontal load are analyzed. The main factors impacting the MSPSW's bearing capacity are examined. Finally, the process of internal force development in boundary members as the drift ratio increases is investigated. The main conclusions are as follows:

(1) Due to the existence of T&L connecting stiffener, the overall stiffness of the MSPSW is increased, and the dimension of single steel plate is reduced, which can be standardized in the factory, and is convenient for processing and transportation. The steel plate in one grid is compressed under the cycle load, the other area is in tension state, which results stable cycling responses and symmetrical shear strength in two directions.
(2) With a reduction in inclined slots width and an increase in slot strips width, the MSPSW's bearing capacity improves. By increasing the cross-sectional dimension of the T&L connecting stiffener and the thickness of the slotted steel plate, the overall mechanical characteristics of the MSPSW are considerably improved.
(3) The setting of T&L connecting stiffener reduces the requirements of MSPSW for the thickness of the out-of-plane concrete panel.
(4) The shear force and bending moment of the beams and columns are significantly decreased as a result of the T&L connection stiffener being adjusted, which allows MSPSW to lower the requirements for the frame members.

Acknowledgements
This work is supported by the National Natural Science Foundation of China (Grant No. 52078092 and 51708073), and Venture & Innovation Support Program for Chongqing Overseas Returnees (No. cx2018036). The financial support is gratefully acknowledged.

Authors' contributions
Shengchao Yang: Investigation, Software, Writing- Original draft. Shuangshuang Jin: Supervision, Methodology, Writing- Reviewing and Editing. All authors have read and agreed to the published version of the manuscript.

Funding
This work is supported by the National Natural Science Foundation of China (Grant No. 52078092 and 51708073), and Venture & Innovation Support Program for Chongqing Overseas Returnees (No. cx2018036). The financial support is gratefully acknowledged.

Availability of data and materials
The datasets are available from the corresponding author on reasonable request.

Declarations

Ethics approval and consent to participate
Not applicable.

Competing interests
The authors declare that they have no competing interests.

Received: 27 January 2023 Revised: 13 March 2023 Accepted: 14 March 2023
Published online: 06 May 2023

References

1. Soong TT, Spencer BF (2002) Supplemental energy dissipation: State-of-the-art and state-of-the-practice. Eng Struct 24(3):243–259
2. Ericksen J. and Sabelli R. (2008) A closer look at steel plate shear walls, Modern Steel Construction, USA. 48(1):63–67
3. Wagner H. (1929) Flat sheet metal girders with very thin metal web, Z.flugtechn.motorluftschiffahrt 20: 200–314
4. Thorburn LJ, Kulak GL, Montgomery CJ (1983) Analysis of steel plate shear walls [R]. Edmonton, Alberta, Canada: Structural Engineering Report No. 107. Department of Civil Environmental Engineering, University of Alberta
5. Caccese V, Elgaaly M, Chen R (1993) Experimental study of thin steel-plate shear walls under cyclic load. J Struct Eng 119(2):573–587
6. Elgaaly M, Liu Y (1997) Analysis of thin-steel-plate shear walls. J Struct Eng 123(11):1487–1496
7. Montgomery CJ, Medhekar M, Lubell AS, Prion H, Ventura CE, Rezai M (2001) Unstiffened steel plate shear wall performance under cyclic loading. J Struct Eng 127(8):973–975

8. Park HG, Kwack JH, Jeon SW, Kim WK (2007) Framed steel plate wall behavior under cyclic lateral loading. J Struct Eng 133(3):378–388
9. Choi IR, Park HG (2008) Ductility and energy dissipation capacity of shear-dominated steel plate walls. J Struct Eng 134(9):1495–1507
10. Kang THK, Martin RD, Park HG, Wilkerson R (2013) Tall building with steel plate shear walls subject to load reversal. Struct Design Tall Spec Build 22(6):500–520
11. Qu B, Guo X, Pollino M, Chi H (2013) Effect of column stiffness on drift concentration in steel plate shear walls. J Constr Steel Res 83:105–116
12. Seismic Provisions for Structural Steel Buildings ANSI/AISC 341–16., American Institute of Steel Construction, Chicago, Illinois, 2016.
13. Technical Specification for Steel Plate Shear Walls JGJ/T 380–2015., Ministry of Housing and Urban Rural Development of the People's Republic of China, Bei Jing, China, 2015.
14. Sun HJ, Guo YL, Wen CB et al (2023) Local and global buckling prevention design of corrugated steel plate shear walls. J Building Eng 68:106055
15. Ghodratian-Kashan SM, Maleki S (2022) Experimental investigation of double corrugated steel plate shear walls. J Constr Steel Res 190:107138
16. Hao J, Li S, Tian W et al (2023) Seismic performance of coupled steel plate shear wall with slits. J Constr Steel Res 201:107674
17. Zhou L, Tan P, Teng X (2023) Experiment and analysis of self-centering semicircular corrugated steel plate shear walls with edge stiffeners. Journal of Building Engineering 66:105876
18. Qiu J, Zhao Q, Yu C et al (2022) Lateral behavior of trapezoidally corrugated wall plates in steel plate shear walls, Part 2: Shear strength and post-peak behavior. Thin Walled Structures 174:109103
19. Jiang ZQ, Yan T, Zhang AL et al (2022) Experimental research on special steel frame with stiffened double steel plate shear wall. J Constr Steel Res 189:107067
20. Shi Y, Luo Z, Xu Y et al (2022) Experimental study on the seismic behavior of high-performance cold-formed steel plate shear walls. Eng Struct 251:113552
21. Guo LH, Rong Q, Ma XB, Zhang SM (2011) Behavior of steel plate shear wall connected to frame beams only. Int J Steel Structures 11(4):467–479
22. Egorova N, Eatherton MR, Maurya A (2014) Experimental study of ring-shaped steel plate shear walls. J Constr Steel Res 103:179–189
23. Jin SS, Ou JP, Liew JYR (2016) Stability of buckling-restrained steel plate shear walls with inclined-slots: Theoretical analysis and design recommendations. J Constr Steel Res 117:13–23
24. Jin SS, Bai JL, Ou JP (2017) Seismic behavior of a buckling-restrained steel plate shear wall with inclined slots. J Constr Steel Res 129:1–11
25. Guo LH, Li R, Rong Q, Zhang SM (2012) Cyclic behavior of SPSW and CSPSW in composite frame. Thin Walled Structures 51:39–52
26. Jin SS, Yang SC, Bai JL (2019) Numerical and experimental investigation of the full-scale buckling-restrained steel plate shear wall with inclined slots. Thin Walled Structures 144:106362

Publisher's Note